SCIREA Journal of Mechanical Engineering

http://www.scirea.org/journal/Mechanical

March 23, 2019

Volume 2, Issue 1, February 2019

# An active forming grinding method for cylindrical involute gears based on a second-order transmission error model

**Gang Li**

Department of Mechanical Engineering, University of Maryland, Baltimore County, Baltimore, MD, USA

## Abstract

An active form-grinding method is proposed to obtain excellent and stable contact performance of cylindrical gears by designing modification forms based on a predesigned controllable second-order transmission error function. First of all, a predesigned second-order transmission error polynomial function is assigned to the gear drive. Mathematical models of modified tooth surfaces that can describe their local deviation and ease-off topography are then obtained with the predesigned second-order transmission error function. Moreover, the form-grinding wheel's profile equation, the coordinate transformation matrix during form-grinding, and settings of computer numerical control form-grinding programs for this active design method can be determined. This approach is ultimately conducted on three involute cylindrical gear pairs to demonstrate its feasibility and effectiveness.

**Keywords**: Cylindrical gears; Second-order transmission error; Active design; Form-grinding

# 1 Introduction

Involute gears, spur and helical ones, are widely applied in gearboxes, planetary gear trains, transmissions and many other industrial applications [1-2]. Evolution of the design and manufacture of such gears by hobbing, shaping, and grinding has been impressive. Geometry, design and manufacture of helical gears was the subject of research represented in the works [3-4] and many others.

Many works are concerned with evaluation of gear contact behavior to improve quality of gear transmission. Kolivand and Kahraman [5] presented a computationally efficient load distribution model for both face milled and face hobbed hypoid gears produced by format and generate process. Fan et al. [6] described a new method to correct tooth flank form errors, utilizing the universal motions and the universal generation model for spiral bevel and hypoid gears. Simon [7] presented a method for the determining an optimal polynomial function for applying the variations to the machine tool setting used in cutting the pinion such that the transmission error of a mismatched spiral bevel gear pair can be reduced. Stadtfeld and Gaiser [8] described the generality of the face hobbing cutting process and applied it to spiral bevel gears. This method is proposed for the direct determination of relations between the pitch cone angles and spiral angles in hypoid gears with face hobbed teeth of uniform depth. Kato and Kubo [9] developed a calculation procedure to determine the tooth bearing and transmission errors of the gears obtained from cutters with different diameter and to clarify the quantitative effects of the cutter diameter on the gear performance.

A methodology was proposed to formate the conjugated pinion tooth flank with a predesigned fourth-order transmission error and path of contact by Wang and Fong [10]. A form-grinding method for cyliderical gears was developed based on a fourth-order TE model [11], and a error sensitivity analysis method was proposed to decribe deviations of contact patterns of tooth surfaces due to misalignments. A real tooth surface This error sensitivity analysis method was used to evaluate mesging performance of a hypoid gear pair in [12]. In order to analyze manufacturing error on tooth surfaces, a modeling approach of digital real tooth surfaces for hypoid gears was developed in [13] based on non-geometric-feature segmentation algorithm. Artoni [14] presented a method to applying corrective machine tool settings to restore the designed functional properties of hypoid gears which contain tooth deviations from theoretical tooth flank during the machining process. Liu et al. [15] proposed an approach to figure out the machine tool settings of a pinion by reverse engineering without having known the theoretical tooth surfaces and the corresponding machine tool settings. Gosselin et al. [16]

presented a method to correct machine tool settings to match a theoretical tooth surface to real tooth surface, which is established by the measurement data. Simon [17] proposed a method to investigate of the tooth contact properties of hypoid gears with different manufacture errors and misalignments.

Application of modern CNC for form grinding method is introduced new concepts in design and formed of involute gears with modifications. The study describes a new function-oriented form grinding method based on a predesigned second-order transmission error function. The proposed method is based on the kinematical modeling of the basic machine settings and motions of a virtual generating rack cutter.

This work focus on the design of gear drives with reduced noise is based on application of a predesigned parabolic function of transmission errors. A predesigned parabolic function of transmission errors absorbs linear functions of transmission errors caused by misalignment, and it is achieved the precontrol on its dynamic performance.

## 2 Functions of Second-Order Transmission Errors

It has been already recognized by researchers that the main source of vibration and noise are transmission errors [1-3]. Reduction of transmission errors and controlling the shape of the function of transmission errors are able to improve the dynamic performance of gear meshing and reduce vibration.

Conventionally, the function of transmission errors can be represented as

$$\Delta\varphi_2 = (\varphi_2 - \varphi_2^{(0)}) - \frac{z_1}{z_2}(\varphi_1 - \varphi_1^{(0)}) \qquad \text{* MERGEFORMAT (1)}$$

where $\varphi_1$ and $\varphi_2$ are the real rotation angles of the driving gear and driven gear, respectively, $z_1$ and $z_2$ are the number of teeth for the driving gear and driven gear, respectively and $\varphi_1^{(0)}$ and $\varphi_2^{(0)}$ are the theoretical rotation angles for the driving gear and driven gear, respectively.

Eq. (1) is a periodic function with period $T=2\pi/z_1$. A predesigned second-order parabolic function of transmission error is applied to reduce or eliminate gear noise and increase gear strength for forming grinding method of involute gears. As shown in Figure.1, the second-order polynomial function is represented as

$$\Delta\varphi_2 = b_0 + b_1\varphi_1 + b_2\varphi_1^2 = \boldsymbol{X}\boldsymbol{Y}^{\mathrm{T}} \qquad \text{* MERGEFORMAT (2)}$$

where $\boldsymbol{X} = [b_0\ b_1\ b_2]^{\mathrm{T}}$ and $\boldsymbol{Y} = [1\ \varphi_1\ \varphi_1^2]^{\mathrm{T}}$. As shown in Figure 1, the geometry of the second-order polynomial function is represented as

$$\varphi_1 = -\delta + T/2, \quad \Delta\varphi_2 = -\varepsilon \qquad \text{* MERGEFORMAT (3)}$$

$$\varphi_1 = -\delta - T/2, \quad \Delta\varphi_2 = -\varepsilon \qquad \text{* MERGEFORMAT (4)}$$

$$\varphi_1 = -\delta, \quad \Delta\varphi_2 = 0 \qquad \text{* MERGEFORMAT (5)}$$

where $\varepsilon$ and $\delta$ are parameters that can be used to control the shape of the second-order polynomial function. Equations (3) - (5) are applied to control the geometric characters of the second-order polynomial function of transmission error $\Delta\varphi_2$. And Eqs. (3)-(5) can be represented in the following matrix form:

$$\boldsymbol{AX} = \boldsymbol{B} \qquad \text{* MERGEFORMAT (6)}$$

where

$$\boldsymbol{A} = \begin{bmatrix} 1 & (-\delta + T/2) & (-\delta + T/2)^2 \\ 1 & (-\delta - T/2) & (-\delta - T/2)^2 \\ 1 & -\delta & \delta^2 \end{bmatrix}, \quad \boldsymbol{B} = \begin{bmatrix} -\varepsilon \\ -\varepsilon \\ 0 \end{bmatrix}$$

The coefficient vector $\boldsymbol{X}$ can be solved as follows:

$$\boldsymbol{X} = \boldsymbol{A}^{-1}\boldsymbol{B} \qquad \text{* MERGEFORMAT (7)}$$

Substituting Eq. (7) into Eq. (2) yields

$$\Delta\varphi_2 = \boldsymbol{A}^{-1}\boldsymbol{B}\boldsymbol{Y}^{\mathrm{T}} \qquad \text{* MERGEFORMAT (8)}$$

By substituting Eq. (8) into Eq. (1), the rotation angle of the driven gear $\varphi_2$ can be represented as

$$\varphi_2 = \boldsymbol{A}^{-1}\boldsymbol{B}\boldsymbol{Y}^{\mathrm{T}} + \frac{z_1}{z_2}\varphi_1 \qquad \text{* MERGEFORMAT (9)}$$

Equation (9) is the constraint equation of the rotation angle of the driving gear $\varphi_1$ and the rotation angle of the driven gear $\varphi_2$. As long as the rotation angles $\varphi_1$ and $\varphi_2$ are restrained by Eq. (9), the gear pair is able to reproduce the predesigned second-order polynomial function of transmission error $\Delta\varphi_2$.

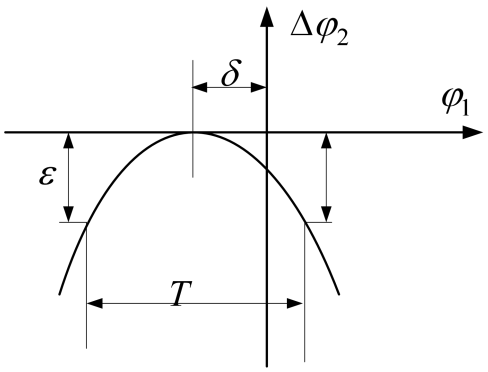


**Figure 1. The second-order function of transmission error.**

# 3 Model of the Hypothetical Generator

## 3.1 Hypothetical generating rack cutter

Based on the theory of gearing, the involute tooth face can be generated by a rack cutter with a planar tooth face. As shown in Figure 2, the generating rack cutter translates horizontally when the generated gear rotates about a fixed axis. The reference circle of the gear rolls without sliding with respect to the pitch line of the rack cutter. Coordinate systems $S_a(x_a, y_a, z_a)$ and $S_b(x_b, y_b, z_b)$ are applied to connect rigidly to the generating rack cutter. $S_c(x_c, y_c, z_c)$ is the movable coordinate system. The position vector and the unit normal vector of the hypothetical generating rack cutter are represented as follows:

$$\boldsymbol{r}_c(u_c, l_c) = \begin{bmatrix} u_c \cos\alpha_n + a_c u_c^{\,2} \sin\alpha_n - d_p \cos\alpha_n \\ \left(u_c \sin\alpha_n - a_c u_c^{\,2} \cos\alpha_n + a_m - d_p \sin\alpha_n\right)\cos\beta + l_c \sin\beta \\ \left(-u_c \sin\alpha_n + a_c u_c^{\,2} \cos\alpha_n - a_m + d_p \sin\alpha_n\right)\sin\beta + l_c \cos\beta \end{bmatrix}$$

* MERGEFORMAT (10)

$$\boldsymbol{n}_c(u_c) = \begin{bmatrix} \sin\alpha_n - 2a_c u_c \cos\alpha_n \\ -\left(\cos\alpha_n + 2a_c u_c \sin\alpha_n\right)\cos\beta \\ \left(\cos\alpha_n + 2a_c u_c \sin\alpha_n\right)\sin\beta \end{bmatrix} \qquad \text{* MERGEFORMAT (11)}$$

where $u_c$ and $l_c$ are surface coordinates of the generating rack cutter blade, $\beta$ is the spiral angle, $\alpha_n$ is the pressure angle, $a_m$ is half of the face width, $d_p$ is position of the parabolic pole, and $a_c$ is parabolic modification coefficient of the cutter tooth profile.

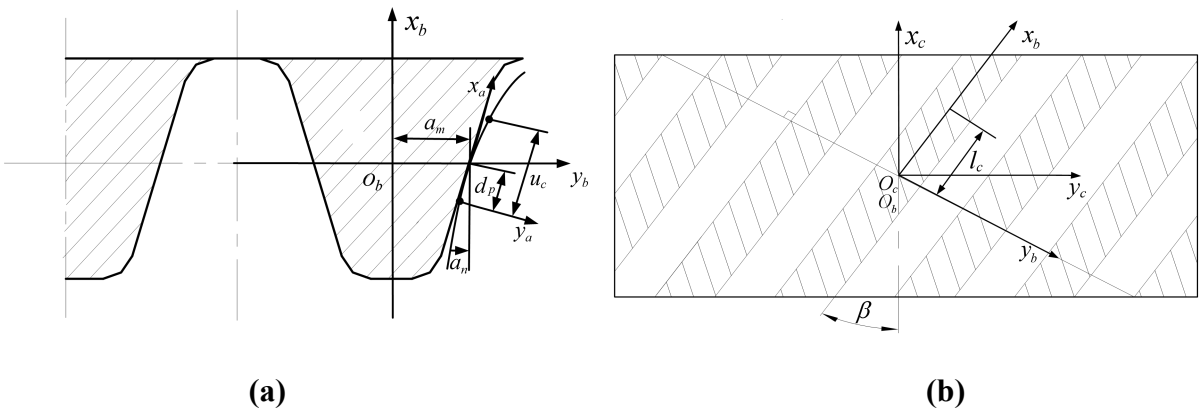


**(a)** **(b)**

**Figure 2. Coordinate systems of the hypothetical generating rack cutter.**

### 3.2 **Mathematical model of the tooth surface of the driving gear**

A general mathematical model for the generation of tooth surfaces of the driving gear is adopted as shown in Figure 3. Coordinate systems $S_m(x_m, y_m, z_m)$ and $S_p(x_p, y_p, z_p)$ are rigidly attached to work piece that is the driving gear in this study. In the coordinate system $S_p$, the driving gear rotates $\varphi_1$, the generating rack cutter moves $r_1\varphi_1$, where $r_1$ is the radius of base circle of the driving gear.

Based on the theory of gearing, the necessary condition for the existence of an envelope to the rack cutter surface can be determined as

$$\frac{X_c - x_c}{\boldsymbol{n}_{cx}} = \frac{Y_c - y_c}{\boldsymbol{n}_{cy}} = \frac{Z_c - z_c}{\boldsymbol{n}_{cz}} \qquad \text{* MERGEFORMAT (12)}$$

where $X_c$, $Y_c$, and $Z_c$ are coordinates of the axis I-I in coordinate system $S_c$ on the generating rack cutter, $x_c$, $y_c$, and $z_c$ are coordinates of the contact point in coordinate system $S_c$, and $\boldsymbol{n}_{cx}$, $\boldsymbol{n}_{cy}$, and $\boldsymbol{n}_{cz}$ are normal vectors of the contact point.

The surface $\Sigma_p$ of the generated driving gear tooth surface is represented as follows

$$\boldsymbol{r}_p(u_c, l_c) = \boldsymbol{M}_{pc}(\varphi_1)\boldsymbol{r}_c(u_c, l_c) \qquad \text{* MERGEFORMAT (13)}$$

$$\boldsymbol{n}_p(u_c, l_c) = \boldsymbol{L}_{pc}(\varphi_1)\boldsymbol{n}_c(u_c, l_c) \qquad \text{* MERGEFORMAT (14)}$$

where $\boldsymbol{M}_{pc}$ and $\boldsymbol{L}_{pc}$ are transformation matrixes from coordinate $S_c$ to $S_p$.

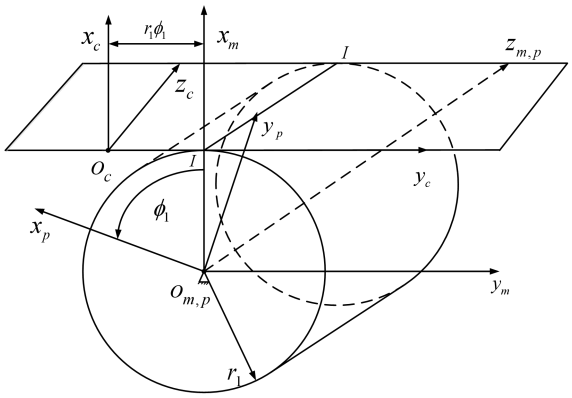


**Figure 3. The coordinate systems of the driving gear.**

### 3.3 **Mathematical model of the tooth surface of the driven gear**

When the driving gear rotates with the angular $\phi_1$, the driven gear is constraint to rotate with the angular $\phi_2$. $\phi_1$ and $\phi_2$ are restrained by Eq.(9).

As shown in Figure 4, the tooth surface $\Sigma_p$ of the driving gear is regarded as the generating surface of the tooth surface $\Sigma_g$ of the driven gear. In $S_g$, $\Sigma_p$ forms a family of surfaces the position vector of which can be determined by

$$\begin{cases} \mathrm{r}_g\left(u_c,\phi_2\right)=\mathrm{M}_{gp}\left(\phi_1\right)\mathrm{r}_p\left(u_c,l_c\right) \\ \mathrm{n}_g\left(u_c,\phi_2\right)=\mathrm{L}_{gp}\left(\phi_1\right)\mathrm{n}_p\left(u_c,l_c\right) \end{cases} \qquad \text{* MERGEFORMAT (15)}$$

where $\boldsymbol{M_{gp}}$ and $\boldsymbol{L_{gp}}$ are transformation matrixes from coordinate $S_p$ to $S_g$.

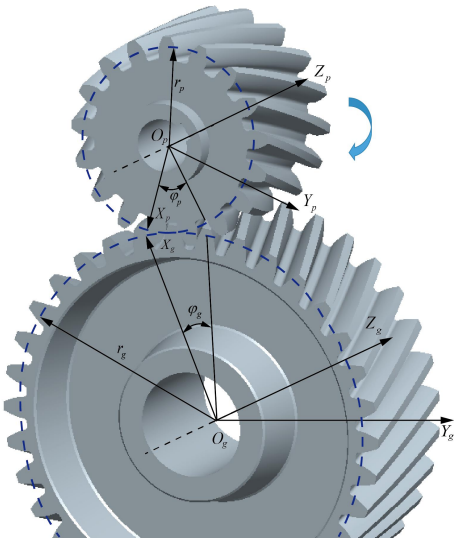


**Figure 4. The coordinate systems of the driven gear.**

# 4 Determination of the Grinding Wheel with the Second Order Transmission Error

In the form grinding progress of helical gears, the contact line between the surface $\Sigma_w$ of the grinding wheel and the surface of the workpiece (the gear) is a space spiral curve. The formation of the forming grinding wheel surface $\Sigma_w$ is achieved by the contact line rotary around the grinding wheel axis. Therefore, according to the relationship of the relative position and movement between the grinding wheel and the gear, the coordinate system $S_w(x_w, y_w, z_w)$ is established, as shown in Figure 5.

## 4.1 Coordinate systems of the form grinding wheel

As shown in Figure 5, coordinate systems $S_w(x_w, y_w, z_w)$ and $S_g(x_g, y_g, z_g)$ rigidly connect the form grinding wheel and the driven gear, respectively; $Z_g$-axis is the rotation axis of the driven gear, and $Z_w$-axis is the rotation axis of the from grinding wheel, $a$ is the center distance, $\Sigma$ is the included angle between $Z_g$-axis and $Z_w$-axis. The transformation relationship between coordinate $S_g$ and $S_w$ is represented as

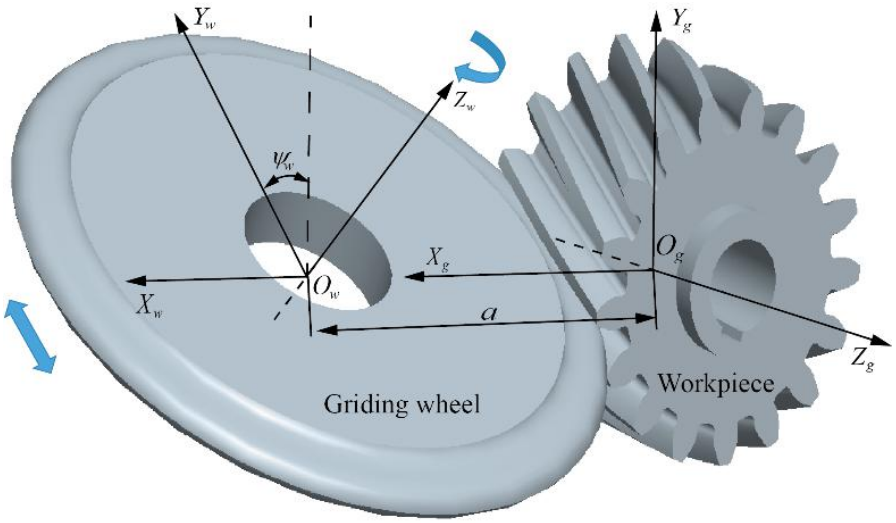


**Figure 5. Coordinate systems of the form grinding wheel.**

$$\begin{cases} X_w = a - X_g \\ Y_w = -Y_g \cos\Sigma - Z_g \sin\Sigma \\ Z_w = -Y_g \sin\Sigma + Z_g \cos\Sigma \end{cases} \quad \text{* MERGEFORMAT (16)}$$

### 4.2 **The mathematical model of the form grinding wheel**

The position that the helicoid grinding wheel surface and the workpiece tangent contact is along the contact line. Therefore, based on the theory of gearing, the necessary constraint to normal vector $\boldsymbol{n_g}(u_c, \phi_2)$ and the relative velocity $\boldsymbol{v_{gw}}$ is

$$\boldsymbol{n}_g(u_c,\phi_2)\cdot \mathrm{v}_{gw}=0 \qquad \text{* MERGEFORMAT (17)}$$

where

$$\boldsymbol{n}_g(u_c,\phi_2)=\begin{bmatrix}\boldsymbol{n}_{xg}\\ \boldsymbol{n}_{yg}\\ \boldsymbol{n}_{zg}\end{bmatrix}=\boldsymbol{L}_{pc}(\phi_1)\begin{bmatrix}\sin\alpha_n\\ -\cos\alpha_n\cos\beta\\ \cos\alpha_n\sin\beta\end{bmatrix} \qquad \text{* MERGEFORMAT (18)}$$

In the coordinate system $S_w$, projections of the angular velocity $\boldsymbol{\omega}$ of form grinding wheel rotation on coordinate axis are

$$\omega=\begin{pmatrix}0 & -\omega\sin\Sigma & \omega\cos\Sigma\end{pmatrix}^{\mathrm{T}} \qquad \text{* MERGEFORMAT (19)}$$

With Eqs.(16)-(19), one has

$$(Z_g+Y_g\cdot\cot\Sigma)\cdot \mathrm{n}_{xg}-(X_g-a)\cdot(\mathrm{n}_{yg}\cdot\cot\Sigma+\mathrm{n}_{zg})=0$$

* MERGEFORMAT (20)

There are two parameters in Eq.(20), $u_c$ and $\phi_2$. Based on Newton-Raphson Method, we generate the discrete points recursively by choosing step size $\Delta u_c$, $\Delta\phi_2$ respectively. The section profile of the form grinding wheel is formed by these discrete points, as shown in Figure 6.

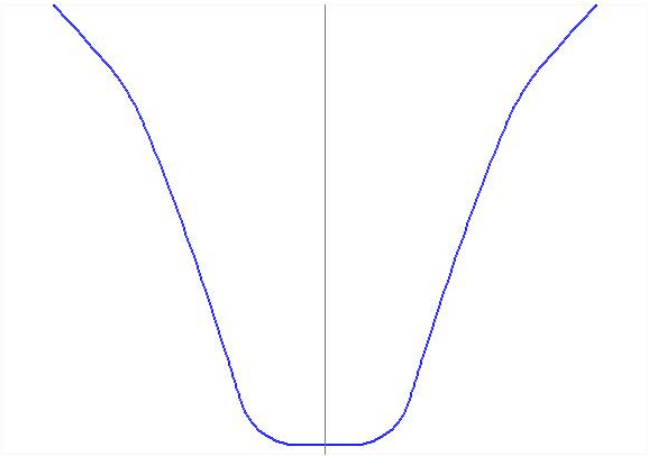

**Figure 6. Section profile of the form grinding wheel.**

## 5 Case Study

In order to verify the consistency between actual transmission error and predesigned transmission error of the form grinding gear. Three examples of numerical analysis are shown in Table 1.

**Table 1. Settings of parameters for numerical analysis.**

| Parameters | Example 1 | Example 2 | Example 3 |
|---|---|---|---|
| $z_1$ | 31 | 31 | 31 |
| $z_2$ | 81 | 81 | 81 |
| $m_n$ / (mm) | 3 | 3 | 3 |
| $\alpha_n$ / (°) | 20 | 20 | 20 |
| $\beta$ / (°) | 15 | 15 | 15 |
| $\varepsilon$ / (″) | 3.873 | 2.502 | 2.476 |
| $T$ / (rad) | 0.203 | 0.203 | 0.203 |
| $\delta$ / (rad) | 0.000 | 0.000 | 0.000 |

**Table 2. The modification coefficients**

| Parameters | $a_{c1}$ | $a_{c2}$ |
|---|---|---|
| Case 1 | 0.002 | 0.000 |
| Case 2 | 0.0025 | -0.0015 |
| Case 3 | 0.002 | -0.001 |

Based on second-order predesigned of involute gear transmission error method, the modification coefficients of the numerical analysis can be obtained, as shown in Table 2. And according to the forming algorithm for section profile of grinding wheel, we can complete forming grinding process of examples in Table 1, as shown in Figure 7.

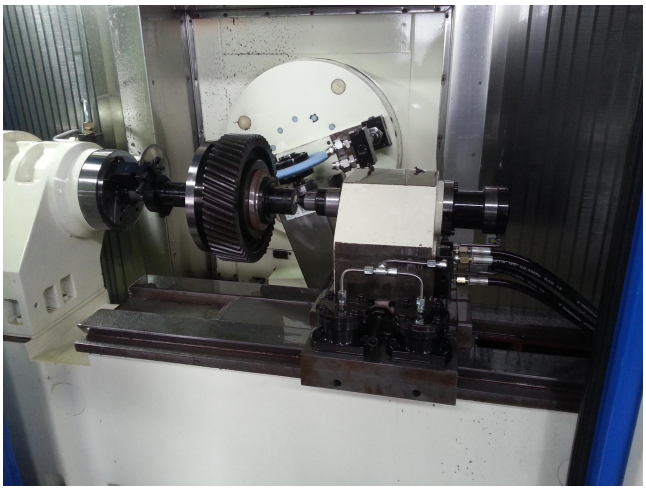

**Figure 7. The form grinding testing.**

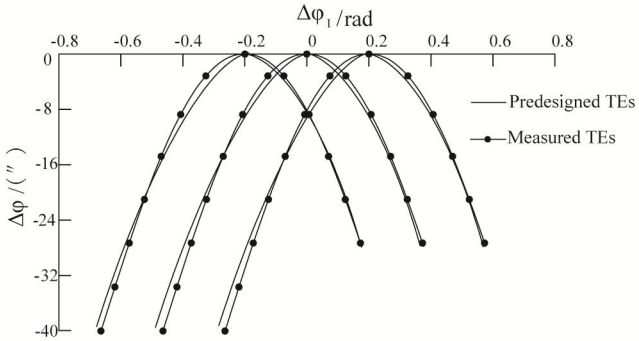


**Figure 8. The comparison for transmission errors of Case 1.**

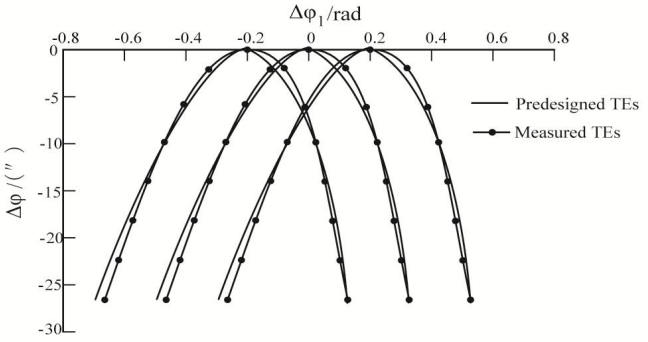


**Figure 9. The comparison for transmission errors of Case 2.**

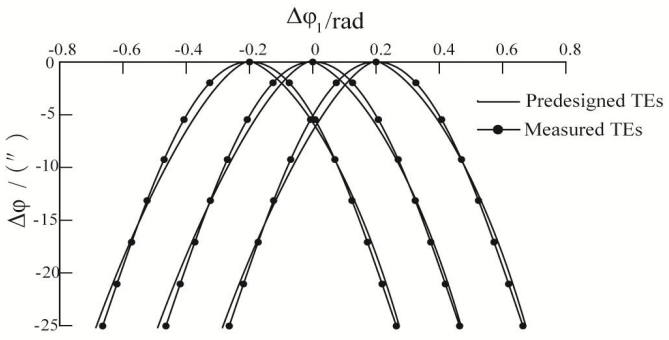


**Figure 10. The comparison for transmission errors of Case 3.**

According to the above method, the numerical analysis results are shown in Figures 8-10. The maximum error among the predesigned transmission error curve and the numerical analysis results is 1.19 ". Through the predesigned transmission error, we can realize to contain complex modification request of involute gear design, and achieving the precontrol on its dynamic performance.

## 6 Conclusions

In principle, the function-oriented form grinding method for involute gears proposed in this paper that based on the predesigned second-order transmission error, is not limited to the involute tooth profile, and is applicable to all types of gears. Because of the light load cases can reflect more gear noise problems. Especially, involute gears with time-varying meshing stiffness are difficult to adjust amount of modification. Therefore, on the basis of the obtained results, the following conclusions can be made:

1. By the predesigned second-order transmission error function, it is realized with very complex modification conditions forming grinding involute gear tooth modification process parameters adjustment.

2. Through a hypothetical generative algorithm by a generating rack, the mathematical model of the section profile of the form grinding wheel is realized based on the second-order transmission error.

3. The advantage of application of a predesigned parabolic function of transmission errors is confirmed by numerical analysis of the transmission errors caused by typical function of transmission errors of gear drives. This can be achieved ahead of the manufacturing process of a designed gear drive.

## References


[1] Litvin, F.L. & Fuentes, A. 2004. *Gear geometry and applied theory*, 2nd edn. New York, NY: Cambridge University Press.

[2] Li, G., Wang, Z. H., and Zhu, W. D., 2018, "Prediction of Surface Wear of Involute Gears Based on Revised Fractal Theory," *ASME Journal of Tribology*, 141(3), p. 031603.

[3] Litvin, F.L., Fuentes, A., & Hayasaka, K. 2006. Design, Manufacture, Stress Analysis, and Experimental Tests of Low-Noise High Endurance Spiral Bevel Gears. *Mechanism and Machine Theory*, 41(1): 83-118.

[4] Lee, C. K. 2009. Manufacturing Process for a Cylindrical Crown Gear Derive with a Controllable Fourth Order Polynomial Function of Transmission Error. *Journal of Materials Processing Technology*, 209(1): 3-13.

[5] Kolivand, M., & Kahraman, A. 2009. A load distribution model for hypoid gears using ease-off topography and shell theory. *Mechanism and Machine Theory*, 44(10): 1848–1865.

[6] Fan, Q., DaFoe, R.S., & Swanger, J.W. 2009. Higher order tooth flank form error correction for face-milled spiral bevel and hypoid gears. *Trans ASME Journal of Mechanical Design*, 130(7): 072601.

[7] Simon, V. 2009. Design and manufacture of spiral bevel gears with reduced transmission errors. *Trans ASME Journal of Mechanical Design*, 131(4): 041007.

[8] Stadtfeld, H.J., & Gaiser, U. 2000. The ultimate motion graph. *Trans ASME Journal of Mechanical Design*, 122(3): 317-322.

[9] Kato, S., & Kubo, A. 1999. Analysis of the effect of cutting dimensions on the performance of hypoid gears manufactured by the hobbing process. In: *4th World Congress on Gearing and Power Transmissions*, Paris, France, March 1999, pp. 585–594.

[10] Wang, P.Y., & Fong, Y.H. 2006. Fourth-order kinematic synthesis for face-milling spiral bevel gears with modified radial motion (MRM) correction. *Trans ASME Journal of Mechanical Design*, 128(2): 457–467.

[11] Li, G., Wang, Z. H., Zhu, W. D., and Kubo, A., 2017, "A Function-Oriented Active Form-Grinding Method for Cylindrical Gears Based on Error Sensitivity," *International Journal of Advanced Manufacturing Technology*, 92(5-8), pp. 3019–3031.

[12] Li, G., Wang, Z. H., and Kubo, A., 2017, "Error-Sensitivity Analysis for Hypoid Gears Using a Real Tooth Surface Contact Model," *Proceedings of the Institution of Mechanical Engineers Part C - Journal of Mechanical Engineering Science*, 231(3), pp.

507–521.

[13] Li, G., Wang, Z. H., and Kubo, A., 2016, “The Modeling Approach of Digital Real Tooth Surfaces of Hypoid Gears Based on Non-Geometric-Feature Segmentation and Interpolation Algorithm,” *International Journal of Precision Engineering and Manufacture*, 17(3), pp. 281-292.

[14] Artoni, A., Gabiccini, M., & Kolivand, M. 2013. Ease-off based compensation of tooth surface deviations for spiral bevel and hypoid gears: Only the pinion needs corrections. *Mechanism and Machine Theory*, 61: 84–101.

[15] Liu, G.L., Chang, K., & Liu, Z.L. 2013. Reverse engineering of machine-tool setting with modified roll for spiral bevel pinion. *Chin J Mech Eng-EN*, 26(3): 573–584.

[16] Gosselin, C., Shiono, Y., Kagimoto, H., & Aoyama, N. 1999. Corrective machine settings of spiral-bevel and hypoid gears with profile deviations. In: *4th World Congress on Gearing and Power Transmissions*, Paris, France, pp. 543–555.

[17] Simon, V. 2008. Influence of tooth errors and misalignments on tooth contact in spiral bevel gears. *Mechanism and Machine Theory*, 43(10): 1253–1267.